Interfacial reactions for the non-stoichiometric TiB_x/(100)Si system

YOUNG-KI LEE,* JUNG-YUEL KIM, YOU-KEE LEE
Department of Semiconductor Engineering & Science and Engineering Research Institute (SERI), UiDuk University, Kyungju 780-713, Korea
E-mail: yklee@mail.uiduk.ac.kr

GI-SEOG EOM
Division of General Education & SERI, UiDuk University, Kyungju 780-713, Korea

YOUNG-KYU KWON
Department of Electronics Engineering & SERI, UiDuk University, Kyungju 780-713, Korea

MIN-SANG LEE, CHUL-MIN LIM, DONG-KUN KIM, YOUNG-CHUL JIN
School of New Materials Engineering, Chonbuk University, Chonju 561-756, Korea

DONG-KOO PARK
Department of Electronic Materials Engineering, Suwon University, Suwon 445-743, Korea

In order to evaluate the interfacial reactions in the TiB_x/(100)Si system and the thermal stability of non-stoichiometric TiB_x films ($0 \leq B/Ti \leq 2.5$), TiB_x/Si samples prepared by a co-evaporation process were annealed in vacuum at temperatures between 300 and 1000°C. The solid phase reactions were investigated by means of sheet resistance, X-ray diffraction, transmission electron microscopy, X-ray photo-electron spectroscopy, and stress measurement. For TiB_x samples with a ratio of $B/Ti \geq 2.0$, an apparent structural change is not observed even after annealing at 1000°C for 1 h. For samples with a ratio of $B/Ti < 2.0$, however, there are two competitive solid phase reactions: the formation of a titanium silicide layer at the interface and the formation of a stoichiometric TiB_2 layer at the surface, indicating the salicide (self-aligned silicide) process. The sheet resistance and the film stress in the Ti/Si and TiB_x/Si systems are well explained by the solid phase reactions.
© 2002 Kluwer Academic Publishers

1. Introduction

The borides of transition and rare-earth metals are primarily considered for application as wear- and corrosion-resistant, decorative coatings on cutting tools and engineering components to increase the lifetime or to lend an attractive surface finish [1–4]. Boride thin films have also been shown to have potential microelectronics applications as a diffusion barrier and a boron diffusion source [5–8]. In particular, titanium boride (TiB_x) is an interesting material for VLSI applications in metallization schemes because of the high thermal stability and low bulk resistivity [8]. The thermal expansion coefficient of bulk TiB_2 is 4.6×10^{-6} K^{-1} which is close to Si (2.5×10^{-6} K^{-1}). It may thus be possible to deposit TiB_x films on silicon with very low stress. Furthermore, TiB_x films that varied from titanium-rich to boron-rich have been shown to be useful in many applications for microelectronic devices. For example, boron-rich TiB_x ($x > 2.0$) films are considered for application as a boron diffusion source into p-type Si. Titanium-rich TiB_x ($x < 2.0$) films, on the other hand, are expected to form the TiB_2/$TiSi_2$/Si contact by a simple post-annealing process, as shown in the Ti-rich TiN_x/Si system, which favors the formation of a low contact resistance and good adhesion to the Si substrate. This type of silicide fabrication allows the formation of a silicide in a desired location without the need for an additional lithographic step.

The purpose of this paper is to examine the thermal stability of non-stoichiometric TiB_x films ($0 \leq B/Ti \leq 2.5$) and the interfacial reactions in the TiB_x/(100)Si system as a result of vacuum annealing. The non-stoichiometric TiB_x films were deposited by a co-evaporation process that allows the composition to be varied from titanium-rich to boron-rich. The characteristics of as-deposited and annealed TiB_x/(100)Si samples were then investigated by means of resistance measurement, X-ray diffraction (XRD), transmission electron microscopy (TEM), X-ray photo-electron spectroscopy (XPS), and stress measurement.

*Author to whom all correspondence should be addressed.

2. Experimental procedure

P-type silicon wafers, ⟨100⟩ oriented with a resistivity of 8–11 Ω cm, were cut into 25 × 25 mm pieces and used as substrates. The wafers were cleaned with organic solvents, rinsed in distilled water, then immersed in a buffered HF acid solution (5% HF in H_2O) for at least 30 sec in order to remove a thin native oxide layer on the surface, and finally rinsed in distilled water prior to deposition.

TiB_x films were produced by a co-evaporation process which can evaporate of Ti (99.9%, 5 mmϕ rod shape) and B (99.9%, lump shape) sources simultaneously. In this study, Ti and B were co-evaporated by dual-electron-beams. The base pressure of the vacuum chamber was less than 4×10^{-6} Torr, and the substrate temperature was kept constant at 500°C. The boron-to-titanium ratio of the TiB_x film was obtained by adjusting the power applied to the two independent constituents. The typical evaporation rate for titanium was kept constant at 0.63 nm/s at 600 W throughout this work, while the boron evaporation rate was varied from 0 to 0.93 nm/s by adjusting the power in the range 0–800 W. The deposition rate was monitored with a quartz resonator plate. The total thickness of the TiB_x film was measured by surface profilometry (Dektak). The B/Ti ratio, deposition rate and film thickness for the TiB_x films are shown in Table I. The composition of the TiB_x films was determined by electron probe micro-analysis (EPMA) and X-ray photo-electron spectroscopy (XPS) analysis. In order to investigate the thermal stability and the interfacial reaction in the TiB_x/(100)Si system, the samples prepared at various deposition conditions were annealed for 1 h in the temperature range 300–1000°C. During vacuum annealing the base pressure of the annealing system was maintained at 5×10^{-7} Torr.

Transmission electron microscopy (TEM), selected area diffraction (SAD) and X-ray diffraction (XRD) were used to characterize the crystalline structure of the thin films. TEM samples were prepared by ultrasonic cutting 3 mm diameter discs and thinning from the silicon side with mechanical polishing and chemical etching ($HF:HNO_3 = 1:1$). The internal stress of the thin films was calculated by measuring the radius of curvature of the Si substrate using an X-ray Lang camera with a proportional counter [9]. The sheet resistance was measured by a conventional four-point probe equipped with Cu probes, on the specimen of sufficient size (10 × 25 mm^2) to exclude the edge effects.

TABLE I B/Ti ratio, deposition rate and total thickness of non-stoichiometric TiB_x films deposited by dual-electron-beam evaporation

Sample	B/Ti ratio	Deposition rate (Å/s)	Thickness (Å)
S-1	0	6.3	1100
S-2	0.59	7.2	1300
S-3	0.83	8.9	1600
S-4	1.24	9.7	1750
S-5	2.10	10.2	1900
S-6	2.38	11.3	2050

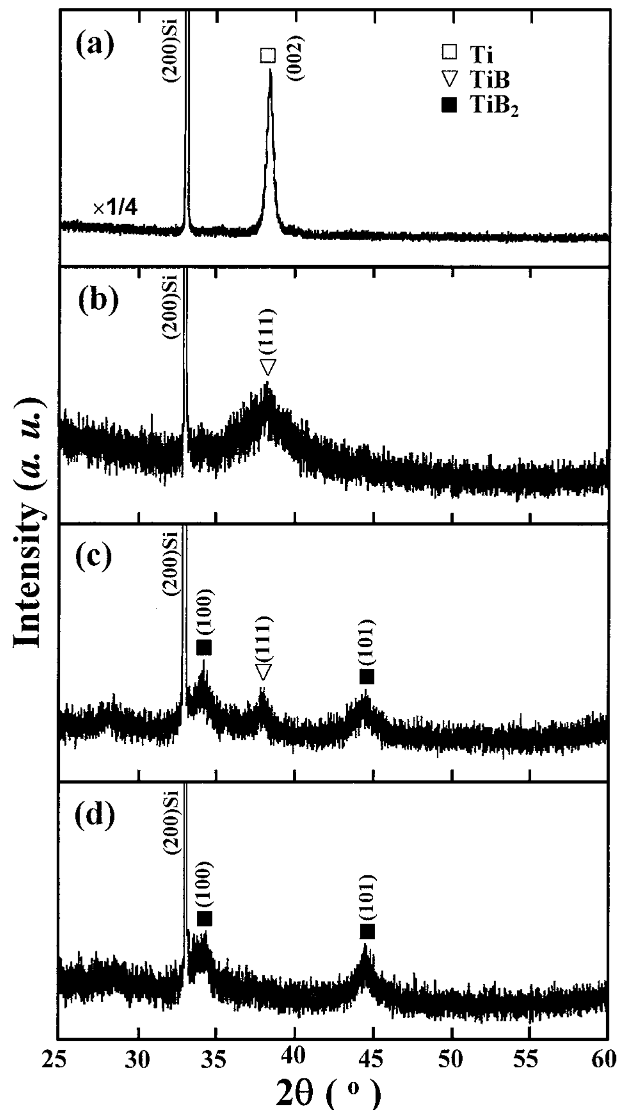

Figure 1 X-ray diffraction patterns for the as-deposited TiB_x/(100)Si samples as a function of boron-to-titanium ratio: (a) pure Ti, (b) B/Ti = 0.59, (c) B/Ti = 1.24, and (d) B/Ti = 2.38.

3. Results and discussion

The XRD patterns for the samples with various boron-to-titanium ratios are shown in Fig. 1. For the pure titanium film, the XRD pattern shows a distinct (002) preferred orientation. For a ratio of B/Ti = 0.59, only single phase TiB with the cubic structure of the ZnS(B3) type, showing a (111) preferred orientation is observed. As the boron concentration increases, however, the TiB_2 phase with the hexagonal structure of AlB_2(C32) type evolves gradually. Samples with a ratio of B/Ti ≥ 2.0 exhibit only single phase TiB_2, indicating the existence of excess boron in these films. The TiB_x spectra show peak broadening. This can arise from very small grain sizes, amorphous region and high residual stresses. The Ti-B-N materials are known to exhibit very broad x-ray diffraction peaks, and the material is often interpreted as being nanocrystalline [10]. As a result of the strong directionality of the covalent boron-boron bonds, boride coatings show a pronounced tendency to form extremely fine-grained to amorphous structures if low-temperature PVD processes are used [11]. In this study, TiB_x films

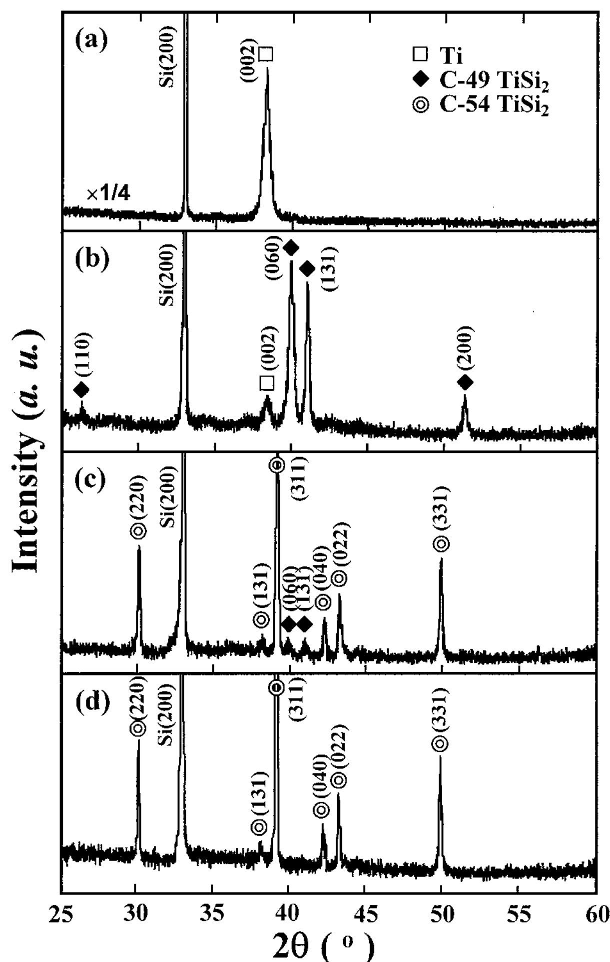

Figure 2 X-ray diffraction patterns for the Ti/(100)Si samples as a function of annealing temperature: (a) as-deposited, (b) 600°C for 1 h, (c) 700°C for 1 h, and (d) 800°C for 1 h.

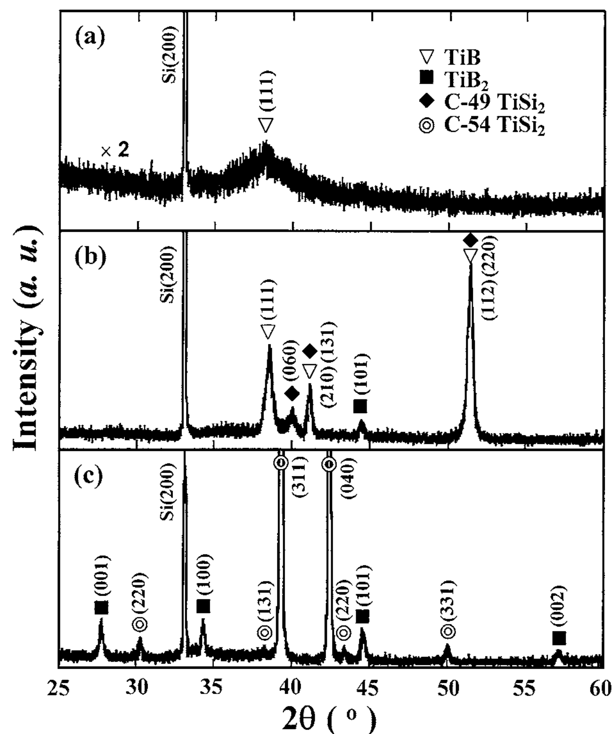

Figure 3 X-ray diffraction patterns for the TiB_x (B/Ti = 0.59)/(100)Si samples as a function of annealing temperature: (a) as-deposited, (b) 600°C for 1 h, and (c) 900°C for 1 h.

deposited at 500°C are polycrystalline. From the XRD peak widths, the crystallite sizes are estimated to be approximately 19 nm for B/Ti = 0.59 and 10 nm for B/Ti = 2.38. This suggests that the grain growth of titanium was impeded by the presence of boron during deposition.

Titanium silicide is formed by the solid phase reaction between titanium and silicon. Two crystallographic structures with minor differences have been proposed for $TiSi_2$. Laves *et al.* [12] found C54 $TiSi_2$ to be face-centered orthorhombic with $a = 8.24$, $b = 4.78$, and $c = 8.54$ Å. Cotter *et al.* [13], on the other hand, found C49 $TiSi_2$ to be base-centered orthorhombic with $a = 3.62$, $b = 13.76$, and $c = 3.605$ Å. In annealed samples, both C49 and C54 $TiSi_2$ phases were found as a function of annealing temperature. Fig. 2 shows the XRD patterns for Ti/(100)Si samples annealed for 1 h in the temperature range 300–1000°C. After annealing at 500°C for 1 h or longer, no silicide or other intermetallic compounds were detected. Above this annealing temperature, however, the titanium film with a distinct (002) preferred orientation rapidly disappeared and Ti reacted with Si to form two kinds of $TiSi_2$: metastable C49 and stable C54. On increasing the temperature to 600°C, the metastable C49 $TiSi_2$ begins to form [Fig. 2b]. At 700°C, the complete conversion of Ti into silicide has occurred and C49 $TiSi_2$ is transformed to stable C54 $TiSi_2$, as shown in Fig. 2c. Finally over 800°C, the C49 $TiSi_2$ phase is completely transformed to stable C54 $TiSi_2$ phase. A similar result for annealed Ti/Si sample has been reported and explained by other researchers [14].

Fig. 3 shows the XRD patterns for TiB_x(B/Ti = 0.59)/(100)Si samples annealed for 1 h in the temperature range 300–1000°C. At temperatures below 500°C, there is no evidence of silicide or other compounds at the Si-TiB_x interface, although the sharpening of TiB_x peaks due to grain growth is observed. On annealing at 600°C for 1 h, however, Ti starts to react with Si to form the C49 $TiSi_2$ and at the same time the single TiB phase transforms to TiB_2, as shown in Fig. 3b. It is considered that there are two competitive solid phase reactions as a result of annealing: the formation of C49 $TiSi_2$ and the formation of stoichiometric TiB_2, indicating the salicide (self-aligned silicide) process. At 800°C, C49 $TiSi_2$ is transformed to stable C54 $TiSi_2$ and the coexistence of TiB and TiB_2 is observed. However, the TiB phase is completely transformed to the TiB_2 phase by annealing at 900°C [Fig. 3c]. In annealed TiB_x/(100)Si sample with $1 \leq B/Ti < 2.0$, the thermal stability of non-stoichiometric TiB_x films and the solid phase reactions in the TiB_x/(100)Si system are similar to those in the annealed B/Ti < 1.0 system. In the samples which are boron-rich (B/Ti ≥ 2.0), on the other hand, an apparent structural change is not observed.

Fig. 4 shows the XRD patterns for the TiB_x(B/Ti = 2.38)/(100)Si samples annealed at various temperatures. As shown in Fig. 4c, even after annealing at 1000°C, an apparent structural change is not observed. By detailed XPS depth analysis, however, it was found that there are two solid phase reactions

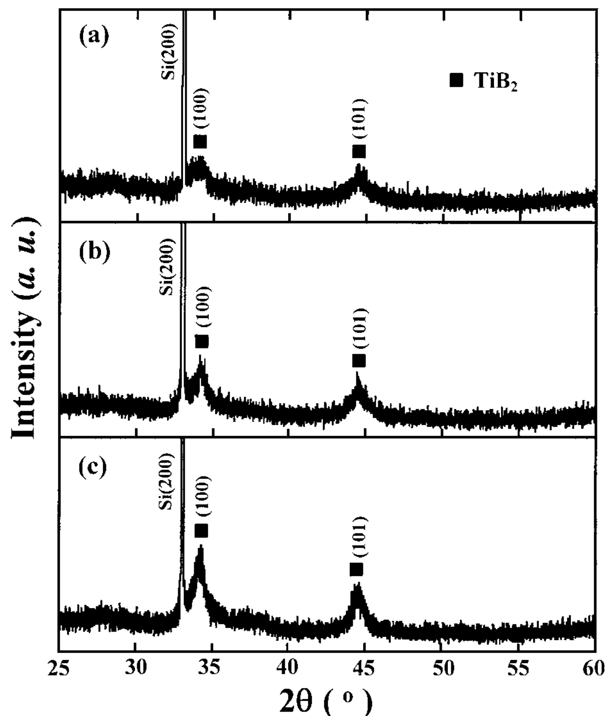

Figure 4 X-ray diffraction patterns for the TiB_x (B/Ti = 2.38)/(100)Si samples as a function of annealing temperature: (a) as-deposited, (b) 700°C for 1 h, and (c) 1000°C for 1 h.

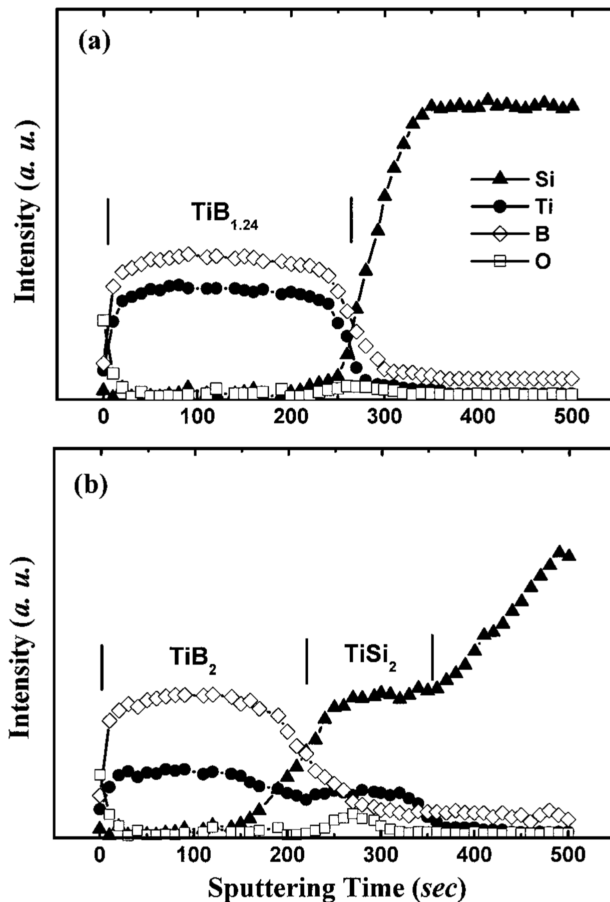

Figure 5 XPS depth profiles for the TiB_x (B/Ti = 1.24)/(100)Si sample: (a) as-deposited and (b) after annealing at 1000°C for 1 h.

taking place, namely, the transformation from non-stoichiometric TiB_x to stoichiometric TiB_2 and the diffusion of B atoms into the Si substrate as a result of the decomposition of boron-rich TiB_x. This makes the boron-rich titanium boride film (B/Ti > 2.0) act as a boron source, doping the underlying silicon substrate during heat treatments. This outdiffusion of boron to the silicon substrate during annealing has been reported by Ryan *et al.* [15].

In order to confirm the interfacial reactions, some samples were analyzed by XPS. Fig. 5a shows the depth profile for the as-deposited TiB_x (B/Ti = 1.24)/(100)Si sample. A relatively high oxygen concentration was observed at the outermost surface due to the contamination formed on the surface of the sample. Also, a small amount of oxygen appears at the boride-silicon interface due to a small amount of interfacial SiO_2. After Ar^+ ion sputtering (7 Å /sec) for over 10 sec, as shown in Fig. 5a, the boron and titanium distributions in the film are fairly uniform from the film surface to the interface, and the boron-to-titanium ratio is close to B/Ti = 1.24, as determined by EPMA. Although the substrate temperature was kept constant at 500°C during deposition, significant inter-diffusion behavior at the Si-TiB_x interface does not occur. Vacuum annealing, on the other hand, creates a wide diffuse region, indicating that a solid phase reaction has occurred at the interface. Fig. 5b shows the depth profile for the TiB_x (B/Ti = 1.24)/(100)Si sample annealed at 1000°C for 1 h. The boride film with a ratio of B/Ti = 1.24 is transformed from the non-stoichiometric to the stoichiometric composition (B/Ti = 2.0). Thus, there is a significant variation in the titanium signal, indicating that excess titanium is consumed during the formation of a silicide at the interface. The composition of the silicide as derived from the XPS profile is close to Ti/Si = 2.0, indicating the C54 $TiSi_2$ phase in accordance with XRD [Fig. 3c]. This indicates that excess titanium retained in the non-stoichiometric TiB_x film reacts with the underlying silicon substrate resulting in the formation of a titanium silicide layer. These results were also confirmed by TEM imaging and SAD patterns.

Fig. 6 shows a SAD pattern and TEM micrograph for the TiB_x (B/Ti = 1.24)/(100)Si sample annealed at 1000°C for 1 h. As shown in Fig. 6a, in addition to the sharp diffraction rings from the stoichiometric TiB_2 phase, many diffraction spots derived from the C54 $TiSi_2$ phase are observed after annealing. This result is in agreement with the results from both XRD and XPS. As shown in the bright-field image [Fig. 6b] taken from the region corresponding to the SAD pattern of Fig. 6a, the grain size of C54 $TiSi_2$ is much larger than that of TiB_2. The TiB_2 layer, the light area in the TEM image, is uniform. However, the grains of C54 $TiSi_2$ (dark areas) are agglomerated. The TiB_x near the surface transforms to stoichiometric TiB_2 by the formation of a titanium silicide at the interface.

The sheet resistance as a function of annealing temperature is shown in Fig. 7. All as-deposited samples exhibit a sheet resistance of between 14–23 Ω/cm. The resistivity, ρ ($=R \times t_f$, R: sheet resistance, t_f: film thickness), increases linearly with increasing boron content in the film. A similar result has been reported for TiB_x films deposited by reactive sputtering in a mixture of argon and 6% diborane [16]. Therefore, it is

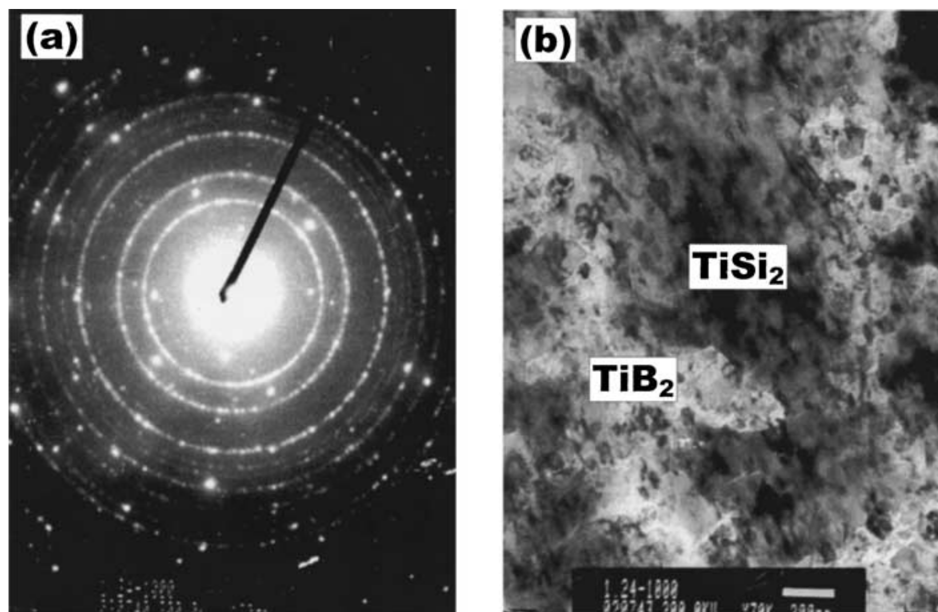

Figure 6 SAD pattern (a) and TEM image (b) for the TiB_x (B/Ti = 1.24)/(100)Si sample annealed at 1000°C for 1 h.

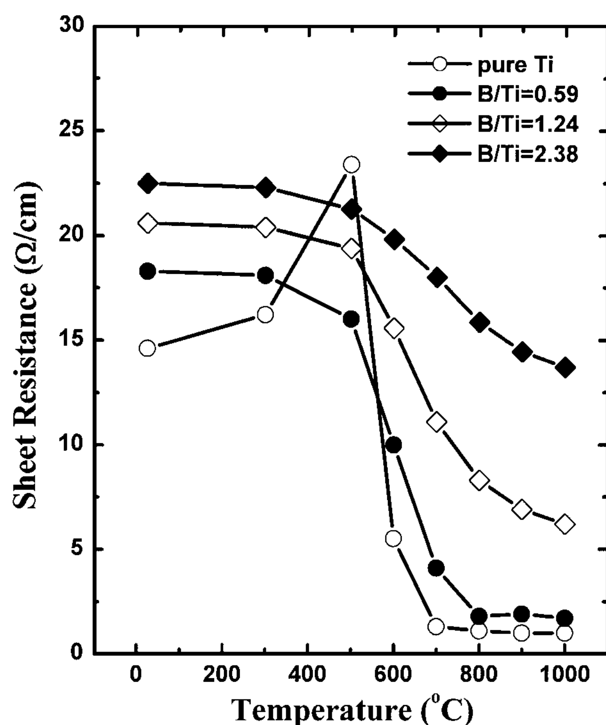

Figure 7 Sheet resistance of the TiB_x/(100)Si samples as a function of annealing temperature. All anneals were carried out in a vacuum of 5×10^{-7} Torr for 1 h.

likely that the resistivity of as-deposited TiB_x films directly correlates with the nominal B/Ti ratio of the film. On annealing, however, the sheet resistance changes as shown in Fig. 7. For the pure Ti film, the sheet resistance increases gradually with temperature until 500°C. The increase in sheet resistance at these low temperatures is most likely caused by impurity effects produced as a result of Si diffusion into the Ti film. At 600°C, however, the sheet resistance decreases steeply due to the formation of a Ti silicide at the interface, as shown in Fig. 2b. At temperatures above 700°C, the sheet resistance is mostly dominated by the formation of C54 $TiSi_2$ on the surface. The sheet resistances of all the annealed TiB_x samples follow similar trends with temperature until 500°C. However, the TiB_x samples annealed above 600°C can be divided into two groups, depending on the sheet resistance. The sheet resistance in the first group (B/Ti < 2.0) decreases abruptly as a result of the formation of TiB_2 on the surface as well as the formation of a Ti silicide at the interface as shown in Fig. 3. On the other hand, the sheet resistance in the second group (B/Ti ≥ 2.0) decreases gradually due to the transformation from non-stoichiometric TiB_x to stoichiometric TiB_2 as shown in Fig. 4. It is suggested that the sheet resistance variation in the annealed TiB_x samples results from the thermal stability of non-stoichiometric TiB_x films and the interfacial reactions in TiB_x/(100)Si system.

Fig. 8 shows the $TiSi_2/TiB_2$ ratio and the sheet resistance of annealed TiB_x/(100)Si samples as a function

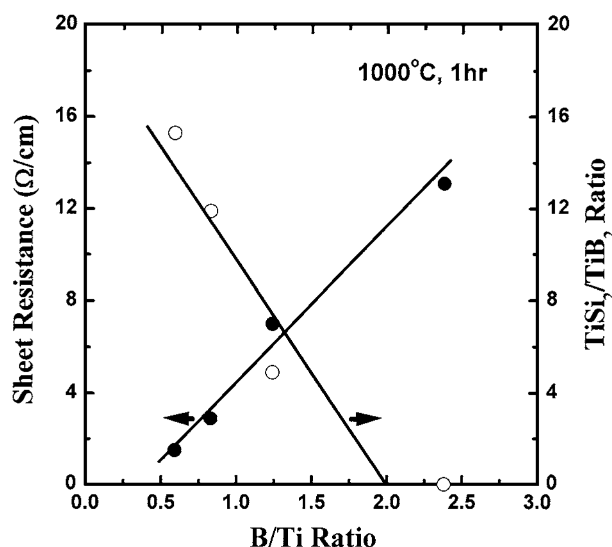

Figure 8 $TiSi_2/TiB_2$ intensity ratio and sheet resistance of the annealed TiB_x/(100)Si samples as a function of boron-to-titanium ratio. All anneals were carried out at 1000°C for 1 h.

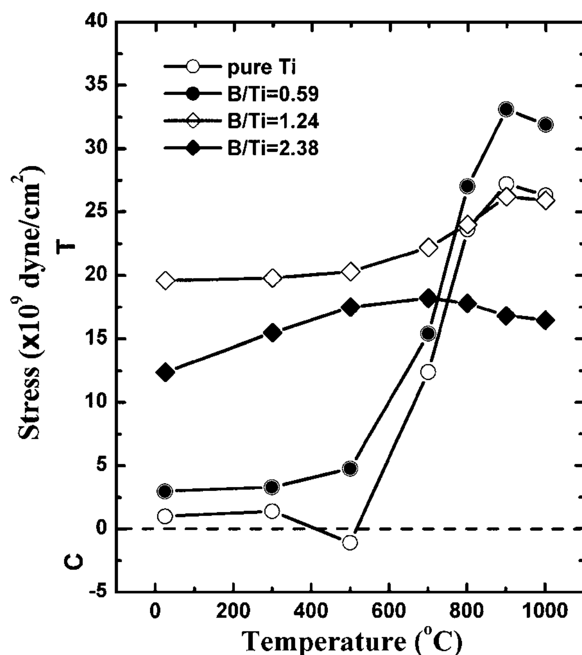

Figure 9 Residual stress of the TiB_x/(100)Si sample as a function of annealing temperature. All anneals were carried out in a vacuum for 1 h.

of B/Ti ratio. All anneals were carried out at 1000°C for 1 h. As shown in Fig. 8, the sheet resistance attained the maximum value in films of $B/Ti \geq 2.0$ that exhibit only single phase TiB_2, and decreased linearly with increasing $TiSi_2/TiB_2$ ratio. The sheet resistance in TiB_x samples with $B/Ti < 2.0$ is due mostly to the formation of a Ti silicide at the interface, although there may possibly be some contribution from factors such as film thickness, grain size, etc.

Fig. 9 shows the variation in film stress of the annealed TiB_x/Si samples as a function of annealing temperature, where T and C refer to tensile and compressive stresses, respectively. The as-deposited Ti/Si sample has a very low tensile stress which does not change significantly up to 400°C. At 500°C, the tensile stress in Ti film changes to a compressive stress due to the diffusion of Si into the Ti layer indicating the atomic peening effect [17]. Above this annealing temperature, the film exhibits a tensile stress. The tensile stress increases with increasing annealing temperature up to 900°C. It is suggested that this is due to the formation of a Ti silicide that is 23 vol% smaller than Ti. All as-deposited TiB_x/Si samples, also, have a tensile stress. The magnitude of the stress in the TiB_x film depends on the nominal B/Ti ratio. It was found that the stress in TiB_x films increases gradually to a maximum value for B/Ti ratio of <2.0, whereas the stresses in TiB_x films with B/Ti ratio of ≥ 2.0 are lower. However, the stress in all the TiB_x films is changed by annealing at 600°C or higher, although the stress does not change significantly up to 500°C.

In the annealed TiB_x sample with $B/Ti = 0.59$, the tensile stress is somewhat higher than that in Ti sample owing to the existence of a TiB_2 layer with a tensile stress, although overall the variation in film stress is very similar to that for pure Ti sample, as known in Fig. 9. Also, the stress changes in the annealed TiB_x/(100)Si samples with $1 \leq B/Ti < 2.0$ are similar to these in for $0 < B/Ti < 1.0$. On the other hand, the stress in the sample with $B/Ti > 2.0$ decreases gradually as a result of the grain growth of the TiB_2 phase as well as the diffusion of excess boron into the Si substrate. The stress variation in Ti/Si and TiB_x/Si systems is well explained by the solid phase reactions.

4. Conclusions

The thermal stability of non-stoichiometric TiB_x films ($0 \leq B/Ti \leq 2.5$) and the interfacial reactions in the TiB_x/(100)Si system have been studied. For the ratio of $B/Ti = 0.59$, only a single phase TiB with a cubic structure of the ZnS(B3) type, showing a (111) preferred orientation, was observed. As the boron concentration increased, however, the amount of the TiB_2 phase with a hexagonal structure of the AlB_2(C32) type increased gradually. Samples with a ratio of $B/Ti \geq 2.0$ exhibit only single phase TiB_2. For TiB_x/Si samples with $B/Ti \geq 2.0$, an apparent structural change is not observed on annealing. For samples with $B/Ti < 2.0$, however, there are two competitive solid phase reactions; the formation of titanium silicide layer at the interface and the formation of stoichiometric TiB_2 layer at the surface, indicating the salicide (self-aligned silicide) process. The sheet resistance in TiB_x films with a B/Ti ratio of <2.0 decreases owing to the formation of stoichiometric TiB_2 on the surface as well as the formation of a Ti silicide at the interface. On the other hand, the sheet resistance in TiB_x films with a B/Ti ratio of ≥2.0 decreases gradually due to the transformation from non-stoichiometric TiB_x to stoichiometric TiB_2. The stress in as-deposited Ti/Si and TiB_x/Si systems is tensile. The stress in annealed samples changes with B/Ti ratio: the tensile stress in samples with $B/Ti < 2.0$ increases owing to the formation of a Ti silicide at the interface, while that in samples with $B/Ti \geq 2.0$ decreases due mostly to the grain growth of TiB_2 phase. The stress variation in Ti/Si and TiB_x/Si systems is well explained by the solid phase reactions.

References

1. A. AGARWAL and N. B. DAHOTRE, *Surface & Coatings Technol.* **106** (1998) 242.
2. J.-E. SUNDGREN and H. T. HENTZELL, *J. Vac. Sci. Technol.* **A4** (1986) 2259.
3. H. O. PIERSON, E. RANDICH and D. M. MATTOX, *J. Less-Common Met.* **67** (1979) 381.
4. P. PESHEV, Z. ZAKHARIEV and K. PETROV, *ibid.* **67** (1979) 351.
5. C. FELDMAN, F. G. SATKIEWICZ and N. A. BLUM, *ibid.* **82** (1981) 183.
6. J. R. SHAPPIRIO, J. J. FINNEGAN, R. A. LUX and D. C. FOX, *Thin Solid Films* **119** (1984) 23.
7. J. R. SHAPPIRIO, J. J. FINNEGAN, R. A. LUX, J. KWIATKOWSKI, H. KATTELUS and M. A. NICOLET, *J. Vac. Sci. Technol.* **A3** (1985) 2255.
8. M. A. NICOLET, *Thin Solid Films* **52** (1978) 415.
9. J. ANGILELLO, F. D'HEURLE, S. PETTERSSON and A. SEGMÜLLER, *J. Vac. Sci. Technol.* **17** (1980) 471.
10. W. GISSLER, *Surf. Coating Technol.* **68/69** (1994) 556.
11. J. E. GREENE, in "Handbook of Crystal Growth," edited by D. T. J. Hurle (Elsevier, Amsterdam, 1993) Vol. 1, p. 640.

12. F. LAVES and H. J. WALLBAUM, *Z. Kristallogr.* **101** (1939) 78.
13. P. G. COTTER, J. H. KOHN and R. A. POTTER, *J. Amer. Ceram. Soc.* **39** (1956) 11.
14. B. W. BOWER, J. W. MAYER and K. N. TU, *Thin Solid Films* **25** (1975) 393.
15. J. G. RYAN, S. ROBERTS, G. J. SLUSSER and E. D. ADAMS, *ibid.* **153** (1987) 329.
16. H.-O. BOLM, S. BERG, M. OSTLING, C. S. PETERSSON, V. DELINE and F. M. D'HEURLE, *J. Vac. Sci. Technol.* **B3** (1985) 997.
17. A. PAN and J. E. GREENE, *Thin Solid Films* **78** (1981) 25.

Received 4 April
and accepted 28 August 2001